

Angular Diameters of α Scorpii and λ Aquarii

P. C. Schmidtke¹

¹*Arizona State University, School of Mathematical and Natural Sciences, PO Box 37100, Phoenix, Arizona, USA 85069-7100*

Abstract. Time-series high-resolution spectra of the cool stars α Scorpii (M1.5 Iab-Ib) and λ Aquarii (M2.5 III Fe-0.5) have been obtained during lunar occultations of these stars, with the goal of measuring the atmospheric extension of prominent photospheric lines. The observed spectral features include the Na I doublet (D lines) and Ca II near-infrared triplet. Using a circular uniform-disk model, the angular diameters within the absorption features have a relative extension, compared to the continuum values, of 55-113% for α Sco and 16-25% for λ Aqr.

1. Introduction

Lunar occultation observations can provide a wealth of information regarding the fundamental properties of cool stars. Extensive campaigns by many observers have yielded angular diameters for a large number of stars (White & Feierman 1987), from which additional parameters, such as the stars' effective temperatures, can be derived. In its simplest form, high-speed time-series photometry of an occultation event is obtained using a single-channel instrument (e.g., Schmidtke & Africano (2011)). The choice of filter is based on many considerations – such as telescope aperture, brightness and spectral type of the star, lunar phase, and specific goals of the observing program. For example, White et al. (1982) observed an occultation of the cool supergiant 119 Tau (spectral type M2 Iab-Ib; Keenan & McNeil (1989)), using a pair of H α filters. They found the angular diameter within the absorption line to be at least twice as large as that from light of the continuum. We present here the results of a study based on occultation observations of cool stars using spectrographs on large telescopes, greatly increasing the number of simultaneously recorded channels. Our goal is to measure the atmospheric extension of prominent photospheric lines at high spectral resolution.

2. Observations

Time-series spectra were recorded during three occultation events, all disappearances behind the moon's dark limb. The bright star α Sco (Antares; spectral type M1.5 Iab-Ib; Keenan & Pitts (1980)) was observed on two occasions, while λ Aqr (spectral type M2.5 III Fe-0.5; Keenan & McNeil (1989)) was observed once. A summary of the occultation events is given in Table 1. For each event the instrument was operated as a "slitless" spectrograph, in which the slit was widened to pass nearly all light from the stellar image. As a result, the spectral resolution depended primarily on seeing conditions. The CCD detector was oriented so that the readout register was parallel to the spectral dispersion (the X-axis) and perpendicular to the spatial direction (the Y-axis). Binning was used in both axes. The minimum sample time was constrained by the CCD's analog-to-digital signal conversion. Hence, there was a compromise between sample time and X-axis binning, with a shorter time being attained at the expense of having fewer spectral elements. Y-axis binning had little effect on the sample time, as multiple (spatial) rows can be quickly collapsed into the readout register. The CCD was read in continuous mode, yielding a data frame with thousands of rows (each a spectrum) by hundreds of columns (each an occultation tracing). An observation lasted 20-30 s, centered on the predicted time of occultation. Sample tracings of two data columns (i.e., channels) for α Sco from Event 1 are shown in Fig. .1. The diffraction fringes are extremely weak because the angular diameter of this star is quite large. The occultation commences earlier and extends later for channel 154 (near the center of the Ca II 8542 Å line) compared to channel 145 (in the continuum). From these tracings alone it is obvious that the size is much larger within the absorption feature.

3. Data Reduction

Our version of the OCCULT reduction program (Peterson, private communication) was modified to process the increased number of channels. The data for each channel were fitted by a circular uniform-disk model with five adjustable parameters: stellar intensity (counts per integration), background intensity, relative time (ms within frame), angular diameter (mas), and rate of motion of the moon's limb ("/s). For occultations of α Sco (Events 1 and 3), the rate was fixed at its predicted value, which assumes the lunar slope at the point of contact to be zero. Attempts to estimate the slope by including the rate as a free parameter were unsuccessful due to weakness of the diffraction fringes. Hence, the angular diameters for α Sco derived here are subject to systematic errors that depend not only on the slope but also the contact angle (CA) of the occultation. These errors scale with the term $\cos(CA \pm \text{slope}) / \cos(CA)$. An unaccounted for 5deg slope can produce systematic errors of 19 and 12% in the modeled diameters for Events 1 and 3, respectively. It is important, therefore, to compare the angular diameters in a relative sense, from one channel to the next (i.e., spectral line vs. continuum). Data from the occultation of λ Aqr (Event 2) show fringes that are moderately resolved, allowing the slope to be estimated. To reduce systematic errors and improve the accuracy of results, a five-parameter fit was made for each channel, which yielded an average rate of -0.3014 ± 0.0125 "/s. This implies a lunar slope of 11.6deg at the point of contact. The data for each channel were then reevaluated with the rate of motion fixed at its average value.

Table 1. Summary of Lunar Occultation Events

	Event 1	Event 2	Event 3
Star	α Sco	λ Aqr	α Sco
Spectral Type	M1.5 Iab-Ib	M2.5 III Fe-0.5	M1.5 Iab-Ib
Telescope ^a	KPNO Mayall	KPNO Mayall	AAT at Siding Spring
Date	1986 July 18	1988 November 18	1990 August 1
UT (predicted)	3:46:11	1:53:59	8:45:13
Position Angle ^b	176.0deg	17.2deg	157deg
Contact Angle ^c	-64.9deg	31.7deg	-52deg
Cusp Angle ^d	9deg S	40deg N	29deg S
Lunar Rate ^e	-0.1727 "/s	-0.3525 "/s	-0.1925 "/s
Spectrograph	RCSP	RCSP	RGO
Camera	UV Fast	UV Fast	82 cm
Grating	B&L #380	B&L #380	1200R
Detector	TI #2	TI #2	Thomson #3
Binning (spatial)	10 pixels	10 pixels	67 pixels
Binning (spectral)	2 pixels (0.94 Å)	3 pixels (1.41 Å)	4 pixels (0.304 Å)
Number of Channels	374	266	255
Sample Time	16.86 ms	11.87 ms	18.3 ms

^aClear aperture of the Mayall telescope is 3.80 m; clear aperture of the AAT is 3.89 m

^bAngle of event around limb of moon, measured from true north

^cAngle of event measured relative to direction of lunar motion; >0 for north of center, <0 for south

^dAngle of event measured from nearest lunar cusp

^ePredicted rate of motion in direction of position angle; <0 for disappearance

4. Results

Plots of modeled stellar intensity and angular diameter for the three events are shown in Figs. .2, .3, and .4, in which prominent spectral features are identified by dashed lines and those channels with bad (CCD column) data are marked by an *. Individual events are discussed below.

4.1 Event 1

α Sco is the third brightest star that can be occulted by the moon. It is a pulsating variable and shows evidence of an asymmetrical brightness profile (Richichi & Lisi 1990). The cool supergiant has a B2.5 V companion that does not affect the observation, as it lies $\sim 2.5''$ from the primary (Mason & Hartkopf 2007) and is >5 mag fainter at the wavelengths of the Ca II near-infrared triplet. Spectra with 16.89-ms sample time were obtained during a lunar occultation visible from Kitt Peak National Observatory. The modeled angular diameters are significantly larger within the absorption features compared to those of the continuum (see Fig. .2). In order to quantify the atmospheric extension of each spectral line, the continuum

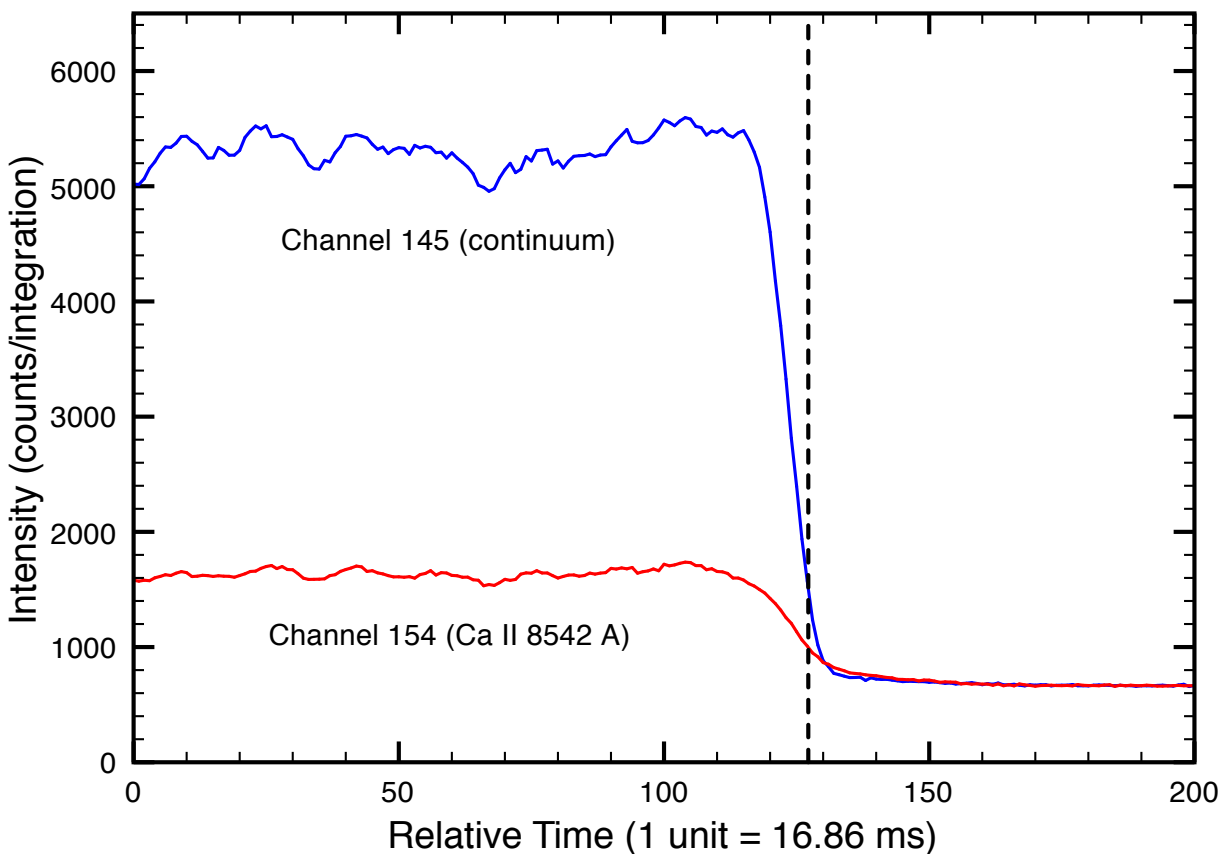


Figure 1: Sample occultation tracings of α Sco from Event 1. Data in channel 154 (red line) are for the approximate center of the Ca II 8542 Å absorption feature, while data from channel 145 (blue line) represent the nearby continuum. The dashed vertical line marks the time of geometric occultation.

diameters, as a function of channel number, were fitted by a second-order polynomial that ranges between 36.9 and 38.3 mas. Relative to this polynomial, the extensions at 8498, 8542, and 8662 Å are 55, 113, and 106%, respectively. These values are similar to that for H α light in 119 Tau (White et al. 1982). The estimated range of continuum diameters is consistent with nearly all published occultation measurements for Antares (Richichi & Lisi (1990); Schmidtke et al. (1991); White & Feerman (1987)) and implies the lunar slope of Event 1 must be close to zero. One exception is the angular diameter of 27.81 ± 0.56 mas found by Schmidtke et al. (1989). It is ironic that this abnormally small measurement was made at the KPNO 0.9 m No. 2 telescope, concurrently with Event 1. The source of the discrepancy is unclear.

4.2 Event 2

An occultation of the cool giant λ Aqr was observed at KPNO, using an instrumental setup almost identical to that of Event 1. To compensate for the higher rate of motion of this event

(>0.3 vs. <0.2 "/s for Event 1) and brightness of the star (~ 3 mag fainter than Antares), the spectral binning was increased to 3 pixels, reducing the sample time to 11.87 ms. The angular diameters of the Ca II absorption lines in λ Aqr show only moderate enhancement over continuum values (see Fig. .3). Applying the same technique as used in Event 1, the relative measures are 17, 16, and 25% for the 8498, 8542, and 8662 Å lines, respectively. The atmospheric extension, therefore, is considerably smaller (as expected) than that found in the supergiant Antares. The fitted continuum diameters lie between 10.5 and 11.8 mas, which are larger than those reported for other lunar occultations of λ Aqr (Schmidtke & Africano (2011); White & Feerman (1987)).

4.3 Event 3

An additional occultation of α Sco was recorded with the Anglo-Australian Telescope at Siding Spring Observatory. The spectral coverage of this event included the strong absorption features of Na I (D lines), and the sample time was 18.3 ms. As shown in Fig. .4, the relative extensions of the angular diameters are 80 and 99% at 5889 and 5896 Å, respectively, when compared to fitted continuum values. These extensions are similar to those for the Ca II features observed in Event 1. The continuum diameters lie between 36.8 and 38.9 mas, a range comparable to the previous occultation of Antares.

5. Comments from the Observing Notebook

Occultation observing is a risky endeavor. Sometimes fate plays a big role. The following notes illustrate how fortunate we were to obtain these data. Referring to Event 1, which was recorded during Arizona's monsoon season, the notes include "Rained during afternoon and evening. Clearing at 8 PM [local time]. Observing at 8:46 PM. First pointed at star <10 min before event." Conditions were more extreme for Event 3, which followed one of the rainiest months on record for New South Wales. The notes state "Got observation through smallest of holes in cloud cover. Had been foggy all afternoon – with some sleet/drizzle at times – after a sunny morning. Fog lifted during hour preceding occultation, but high clouds remained. Some holes during last half hour or so. Largest hole occurred during time of event! Within 10 minutes, however, we were back in the fog!!! Lucky! Lucky! Lucky!"

Acknowledgements. We thank John Africano, Larry Goad, David Allen, Mike Bessell, and Deane Peterson for their contributions to this project. Travel support for the AAT observation was provided by the National Optical Astronomy Observatories.

References

- Keenan, P. C., & McNeil, R. C. 1989, ApJS, 71, 245
Keenan, P. C., & Pitts, R. E. 1980, ApJS, 42, 541
Mason, B. D., & Hartkopf, W. I. 2007, IAU Symposium, 240, 575
Richichi, A., & Lisi, F. 1990, A&A, 230, 355

Schmidtke, P. C., & Africano, J. L. 2011, AJ, 141, 10

Schmidtke, P. C., Africano, J. L., & Quigley, R. 1989, AJ, 97, 909

Schmidtke, P. C., Hopkins, J. L., Africano, J. L., & Walker, A. R. 1991, International Amateur-Professional Photoelectric Photometry Communications, 45, 60

White, N. M., & Feerman, B. H. 1987, AJ, 94, 751

White, N. M., Kreidl, T. J., & Goldberg, L. 1982, ApJ, 254, 670

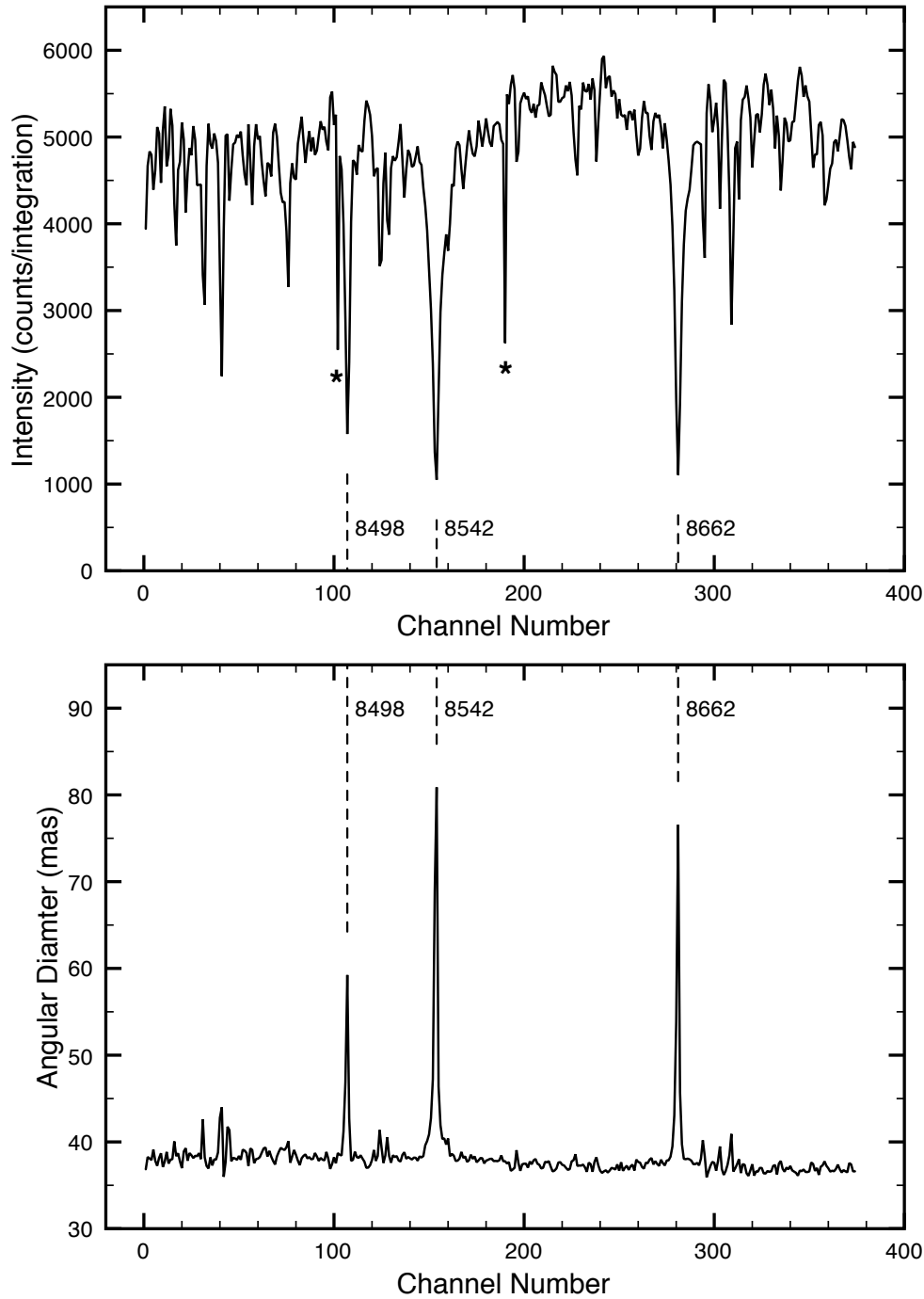


Figure .2: Model results for Event 1, a lunar occultation of α Sco, showing atmospheric extension of the Ca II near-infrared triplet absorption lines. Channels containing bad CCD data are marked with an *.

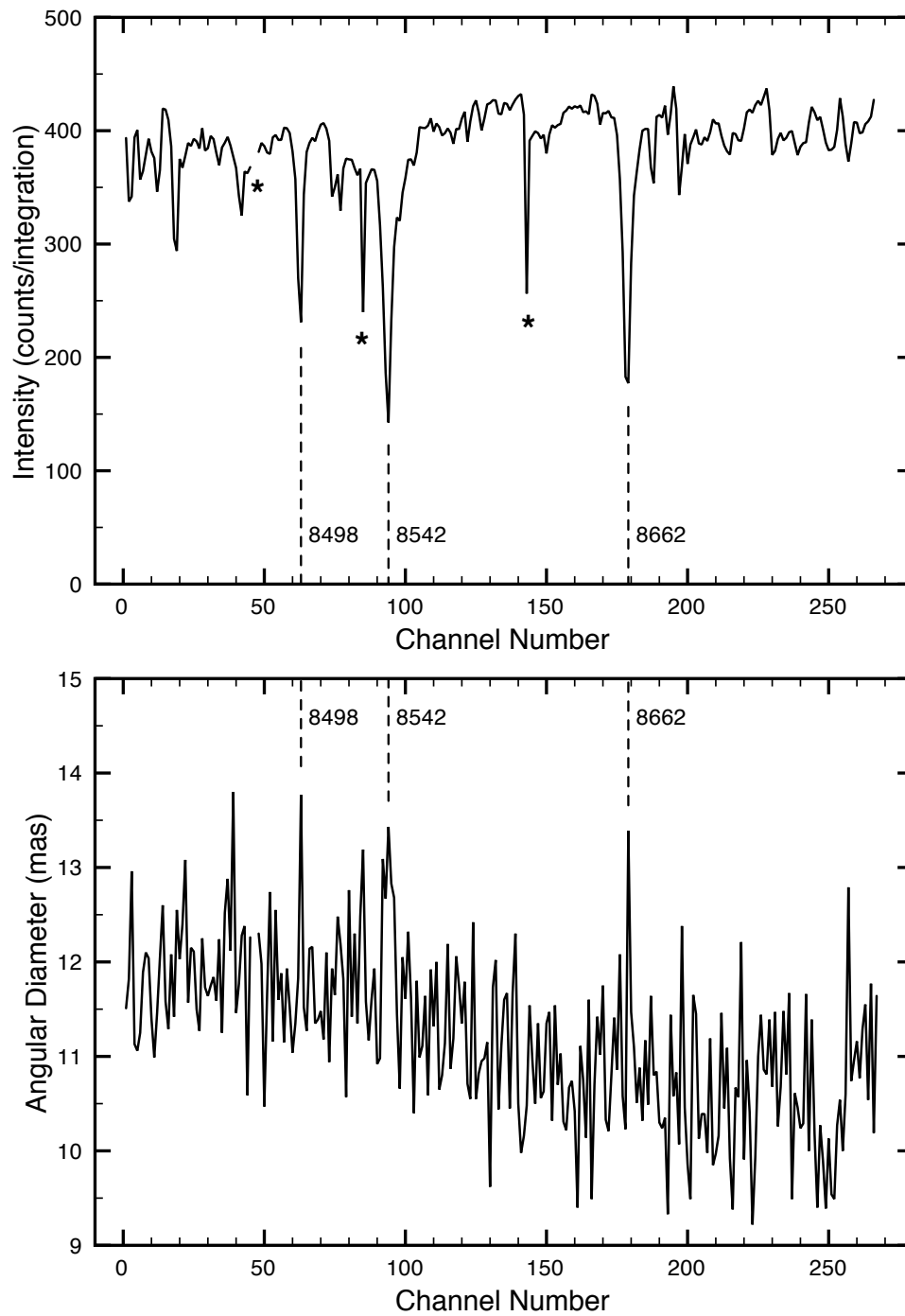


Figure 3: Model results for Event 2, a lunar occultation of λ Aqr, showing atmospheric extension of the Ca II near-infrared triplet absorption lines. Channels containing bad CCD data are marked with an *.

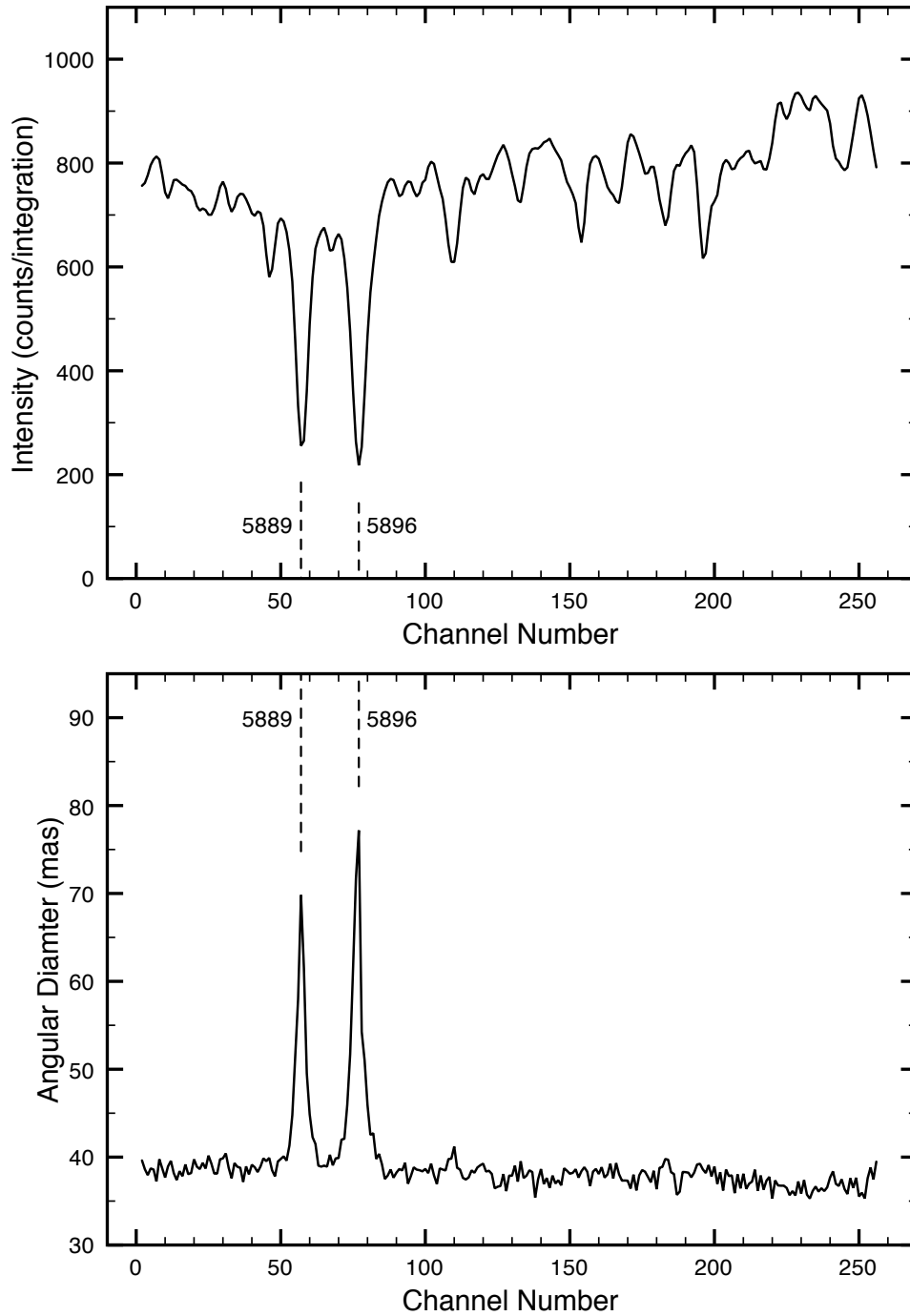


Figure .4: Model results for Event 3, a lunar occultation of α Sco, showing atmospheric extension of the Na I doublet absorption lines.

